Measuring the Stress Dependence of Nucleation and Growth Processes in Sn Whisker Formation

ERIC CHASON[1,2] and FEI PEI[1]

1.—School of Engineering, Brown University, Providence, RI 02912, USA. 2.—e-mail: Eric_Chason@Brown.edu

Sn whiskers/hillocks are believed to form due to stress in the layers, but the dependence on the stress has been difficult to quantify. We therefore used the thermal expansion mismatch between Sn thin films and Si substrates to induce controlled stress by heating. This enables us to measure the average stress in the layer (using wafer curvature) at the same time as we monitor the nucleation rate (using optical microscopy). Scanning electron microscopy of the surface after intervals of heating is also used to quantify the whisker volume as a function of stress and time. The results allow us to determine the dependence of the whisker nucleation rate and the growth rate on the applied stress. They also show that whisker formation is not the dominant mode of plastic strain relaxation in the Sn layer.

INTRODUCTION

It is well known that Pb-free Sn coatings have a tendency to produce whiskers, i.e., long, thin filaments that can cause short circuits and system failures.[1] As documented by NASA on its website,[2] such whiskers have led to satellite crashes, nuclear power plant shutdowns, and recalls of medical devices and consumer electronics. They were even found in the accelerator pedal of Toyota automobiles.[3,4] Whisker-related problems have become more acute since the passage of legislation in Europe mandating the removal of Pb from electronics manufacturing because alloying with Pb suppressed whisker formation in the past.[5]

Although Sn whiskers (and lower aspect ratio features that we refer to as hillocks) have been the object of intense study in recent years,[1] there are still many outstanding questions about what makes them grow and why they grow from specific sites on the surface. To put this in the broader context of materials science, we still do not understand what controls whisker nucleation and what controls their growth. Progress in these areas is needed to be able to predict their formation and develop better mitigation strategies.

Over time, a consensus has emerged that stress is the driving force for whisker/hillock formation.[6–13] In Sn layers coated over Cu conductors, the stress often develops due to the production of intermetallic compounds (IMCs) at the Sn-Cu interface.[7,9,10,14,15]

However, quantitative studies relating whisker formation to the IMC-induced stress are difficult because the stress is difficult to predict and/or control. To gain a better understanding, we have developed a system that enables us to impose stress by using thermal expansion mismatch between the Sn layer and a Si substrate to create strain when the system is heated. The resulting film stress and whisker density are measured simultaneously so that they can be directly correlated. These studies are supplemented by scanning electron microscope (SEM) measurements of the volume of individual features in order to relate the growth rate to the applied stress.

The thermally induced stress[16–18] has enabled us to measure the coevolution of the stress, whisker density, and whisker volume. The results have been used to determine quantitatively how the stress influences the rates of nucleation rate, growth, and plastic strain relaxation. Using classic nucleation theory, we can determine how much the energetic barrier to nucleation decreases due to the applied stress. From this, we propose a mechanism for stress-dependent nucleation that is consistent with our observations. We have also directly measured the dependence of the whisker growth rate on the stress at different temperatures and shown that a critical magnitude of stress is necessary for whiskers to grow. Using the nucleation and growth kinetics, we have been able to determine how much

of the plastic strain can be attributed to whisker formation and how much is due to other strain relaxation processes.

BACKGROUND

It has been known for a long time that stress in Sn layers contributes to whisker/hillock growth.[6,19,20] Although there can be multiple possible sources of stress, the stress induced by IMC formation is persistent and therefore the most likely to lead to long whiskers that can cause failure.

Because whiskers/hillocks only grow from a small number of surface sites (typically less than 10^{-4} of the grains in the film form into whiskers/hillocks), there must be some feature about these sites that makes whiskers initiate there preferentially. Multiple potential underlying factors have been investigated: grain orientation,[7,21] surface defects,[22,23] weak oxide,[8,22,24] IMC pileup,[25,26] and microstructure.[9,11,25,27] Although all may play a role in different systems, the most common feature underlying whiskers/hillocks is that they grow out of grains near the surface. This causes them to have a grain boundary underneath them that is at least partially horizontal in character as seen in focused-ion beam (FIB) cross sections.[11,25,28] It has been pointed out[9,11,27,28] that this enables atoms to be accommodated at the base of the whisker and push material outwards, thus relieving stress in the layer. In comparison, the grain structure of most of the Sn layer is columnar, so adding atoms at these vertical grain boundaries does not relieve stress. The presence of a tenacious oxide on the Sn surface is also important because it prevents diffusion of atoms to the free surface, which could also relieve stress.[10]

Because the grains that whiskers grow out of have horizontal grain boundaries, the root of the whisker/hillock is often found near the surface. However, surface grains or grains with horizontal boundaries are not typically seen in as-grown layers of Sn. Vianco and Rejent[29,30] have suggested that such grains form due to dynamic recrystallization driven by strain energy density in the film. Sarobol et al.[31] have seen such nucleation of new grains in large-grained Sn layers but only after a large number of repeated thermal cycles. Other experimental studies[22,32] have shown that the shape and orientation of the grain that grows into a whisker is the same as in the initial microstructure, suggesting that the whiskering grain is already there after deposition and not newly nucleated. Therefore, there is still significant uncertainly about where the sites come from that turn into whiskers.

EXPERIMENT

One of the difficulties in understanding whisker formation in Sn layers on Cu is the difficulty of controlling the driving force (stress) due to IMC formation. To circumvent this problem, we use thermal expansion mismatch between the Sn layer and a Si substrate to induce stress by heating the sample. The samples consist of 200-μm thick Si substrates that have had 25 nm Ti and 80 nm Cu deposited by electron beam evaporation. A 2.5-μm Sn layer is electrodeposited over the Cu (details of the sample fabrication can be found in Ref. [16]). The Cu layer is used to obtain the same microstructure in the Sn layer as for our other studies of Sn on Cu.

After deposition, the samples are stored in ambient temperature for 9 days to allow the Cu to react fully with the Sn to form IMC. Measurements of the IMC volume versus time[1] indicate that this is a sufficient period for all of the 80 nm of Cu to be consumed; this was confirmed by cross-sectional measurements that showed no remaining Cu layer[16] and by the fact that the stress in the Sn layer due to IMC formation stopped changing. We also measured the IMC structure before and after the thermal stress measurements and found that the IMC morphology did not change. Therefore, we assume that we can attribute the stress changes during the heating treatments to thermal mismatch stress and not to growth or modification of the IMC.

The experimental system that we have developed for these studies is shown schematically in Fig. 1.[16] It allows us to heat the sample and simultaneously measure the stress and whisker formation kinetics using wafer curvature and optical microscopy. Details of the thermal treatments (heating rate, dwell time, maximum temperature, etc.) are discussed for the various experimental studies below. The stress is measured from the polished Si side of the sample using a multibeam optical stress system (MOSS).[33] This technique monitors the curvature in the substrate to determine the average in-plane stress (σ) in the thin film.[34] The system illuminates the sample with an array of parallel laser beams and monitors the deflection of the beams to determine the curvature/stress in real time.

The optical microscope observes the Sn side of the sample through a hole in the heating stage with a light source that illuminates the sample obliquely. Although the resolution is not sufficient to image the whiskers, the light scattered from the surface enables the number of whiskers/hillocks to be observed (after they reach a minimum size of 0.5 μm^3). SEM measurements of the same region of the surface were used to validate the technique for whisker density (further details of the image analysis can be found in Ref. [16]).

SEM was also used to quantify the volume evolution of individual features.[35] Samples were thermally cycled for different intervals (as described below) and then transferred to the SEM and measured after less than 40 min to minimize relaxation. Careful alignment allowed the same features to be monitored over successive heating cycles. The feature volume was estimated from micrographs of the surface and corrected for the angle of observation.
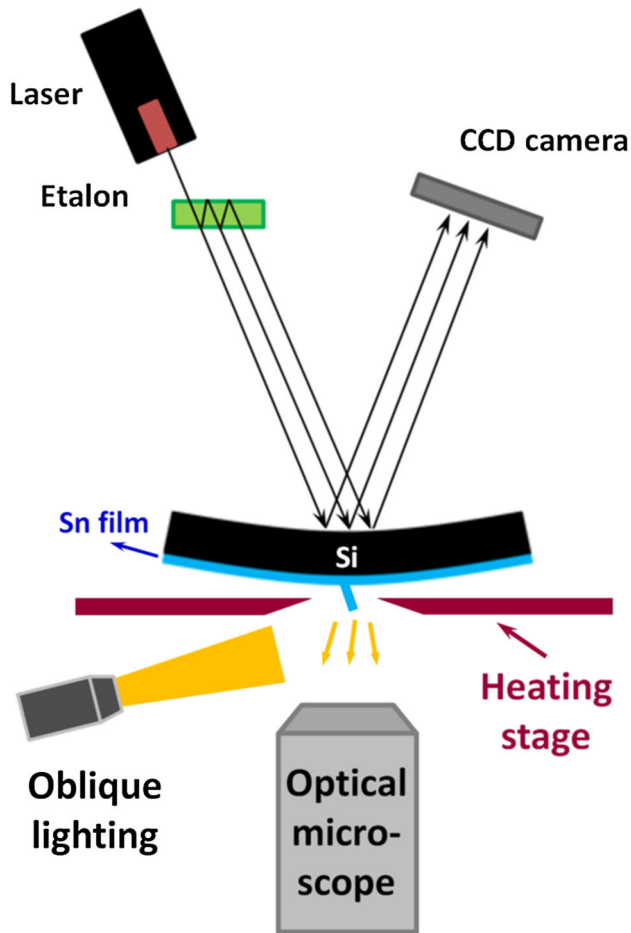
Fig. 1. System for measuring stress and whisker density using thermally induced strain.

The stress was also measured during these heating periods so that the growth rate could be correlated with the stress and temperature.

RESULTS AND DISCUSSION

In the following sections, we describe results from several recent studies that address the kinetics of whisker nucleation, the stress and temperature dependence of the whisker growth rate and the relation between whisker volume and plastic strain. The individual sections include a description of the measurements that were made as well as a discussion of their meaning.

Kinetics of Whisker Nucleation

Measurements of Stress and Whisker Density

Simultaneous measurement of the sample temperature, stress, and whisker density enables us to study how whisker nucleation depends on the stress.[17,18] The results are shown in Fig. 2 for thermal treatments with maximum temperatures of 45°C (Fig. 2a), 55°C (Fig. 2b), 65°C (Fig. 2c) and

75°C (Fig. 2d). In each case, the sample was heated at 2°C/min and then held at the maximum for the duration of the experiment. For each cycle, the stress is initially proportional to the temperature change, which corresponds to elastic deformation in the film. At longer times and higher temperatures, the stress starts to diverge from the thermal strain, indicating the onset of plastic deformation. For the 45°C cycle, this occurs after the final temperature is reached. For the other cycles, the stress starts to relax while the sample temperature is still rising. In all cases, the stress continues to relax while the sample is held at elevated temperature, with a rate that is greater for the higher temperatures. For all the measurements, the stress stops relaxing at approximately −15 MPa, independent of the maximum temperature that was used.

The corresponding measurement of the whisker/hillock density shows how the appearance of whiskers on the surface coincides with an increase in the rate of stress relaxation. The number of whiskers increases rapidly at first, but then the rate of appearance of new whiskers decreases as the stress reaches saturation. The total number of whiskers is larger at the high temperatures than the low temperatures.

The measurements of the whisker/hillock density enable us to quantify the change in the number of whiskers as the thermal stress is applied. The evolution has a sigmoidal shape, increasing rapidly at first and then saturating. These kinetics suggests that the creation of a whisker site may occur by a nucleation process, i.e., the creation of sites in which whiskers form by overcoming an energetic barrier through a process of thermal fluctuations. This is in contrast to other possible mechanisms, such as a critical stress to crack the oxide. In that case, the whisker might be expected to start to grow as soon as the critical value was exceeded.

The time derivative of the density (i.e., nucleation rate) is shown as the dotted line in the bottom row of figures. From our measurements of the stress and density, we can also plot the nucleation rate as a function of the stress. However, because the whiskers have to grow to a size of 0.5 μm^3 before we can observe them, the data has to be corrected for this time lag. We use a model for the whisker growth (described below) as a function of stress and temperature to estimate the time it takes for the whiskers to grow large enough to be observed. This value is on the order 10 min for the measurements at 45°C and 3.5 min for 75°C. This correction has the effect of making the peak in the nucleation rate close to the maximum of the compressive stress.

We show the corrected dN/dt versus stress in Fig. 3a for the different measured temperatures. The nucleation rate is seen to depend strongly on the stress, changing by a factor greater than 10 across the stress range measured. The nucleation rate also depends on temperature, increasing at higher temperature for the same value of the stress.
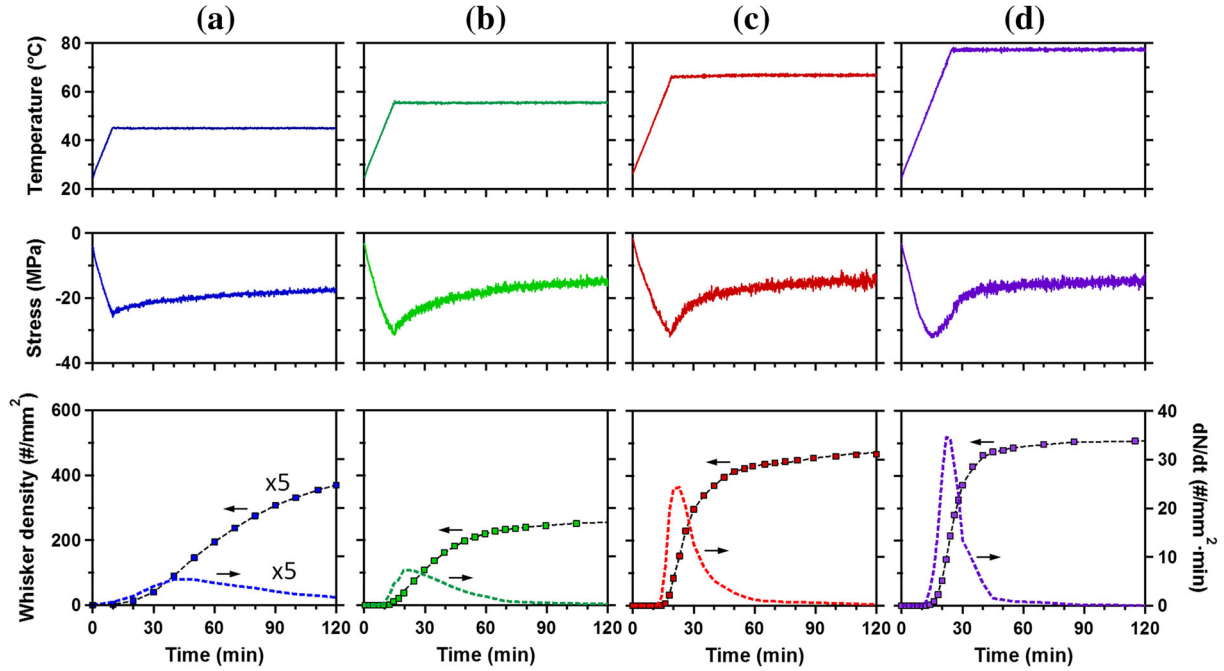
Fig. 2. Measurements of temperature, stress, and whisker density during heating to (a) 45°C, (b) 55°C, (c) 65°C, and (d) 75°C. The lower graph shows the whisker density (left axis) and corresponding nucleation rate (dN/dt) (right axis). The density and nucleation rate at 45°C have been multiplied by 5 to make the data readable. The figure is adapted with permission from Ref. 18.

We analyze these nucleation kinetics in terms of classic nucleation theory to determine the effect of stress on the energetic barrier to nucleation. This can be done without knowing the specific nucleation mechanism leading to whisker site formation. Based on the results, in the following section we propose a mechanism for the nucleation process that is consistent with the measurements.

In classical nucleation theory[36] the nucleation rate depends on

$$\frac{\mathrm{d}N}{\mathrm{d}t} \propto \beta_\mathrm{c}(T)\, \mathrm{e}^{\frac{-\Delta G*}{kT}} \qquad (1)$$

where ΔG^* is the stress-dependent barrier for nucleation and β_c is the rate at which a cluster grows beyond its critical size (which we assume to depend on the temperature but not the stress). We can obtain the dependence of ΔG^* on stress from the measured nucleation rate:

$$\Delta G^* = -kT \ln(\mathrm{d}N/\mathrm{d}t) + \ln(\beta_\mathrm{c}) + \Delta G^*_\mathrm{ref} \qquad (2)$$

where ΔG^*_ref is the barrier height for some reference value of the stress.

We can determine β_c by choosing values that produce the same dependence of ΔG^* on the stress for the measurements at different temperatures. In brief, we do this by using values of β_c that produce the best fit to a second-order polynomial; further details can be found in Ref. 18. When analyzed this way, all the data collapse onto a single curve (shown in Fig. 3b; the polynomial is shown as the dashed line). This figure shows how the nucleation barrier

decreases with higher stress (we use -18 MPa for the reference value because it is the smallest stress at which the nucleation rate could be measured). The values of β_c derived from this method have an Arrhenius temperature dependence with an activation energy 0.85 eV.

Possible Nucleation Mechanism

The kinetics described above suggest that the whiskering sites are formed by a nucleation process. In addition, cross-sectional measurements of the microstructure indicate that the sites where whiskers form are surface grains, i.e., grains with horizontal grain boundaries near the surface. As discussed above, such surface grains are not typically found in the as-deposited samples. However, our measurements of whisker evolution[32] also show that whiskers form out of existing grain orientations, not newly nucleated ones.

These observations at first seem contradictory. How is it possible to have whiskers form out of surface grains that are not initially present without nucleating a new grain? A nucleation mechanism that is consistent with all these observations is described here. Consider an initially columnar microstructure (as shown schematically in Fig. 4a). Under an applied stress, different grains will have different strain energy density. Suppose that the grain in the center of the schematic has higher strain energy density than the surrounding grains. This will lead to strain-assisted grain boundary migration. If the grain boundaries are pinned at the
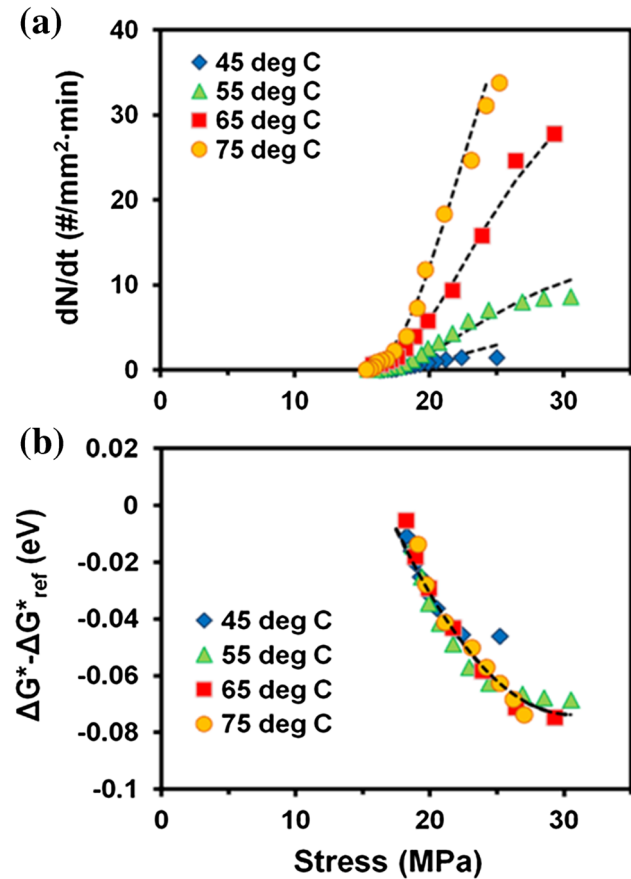
Fig. 3. (a) Nucleation rate versus stress at temperatures indicated in figure. (b) Change in activation barrier for nucleation (ΔG^*) versus stress. The figure is adapted with permission from Ref. 16.
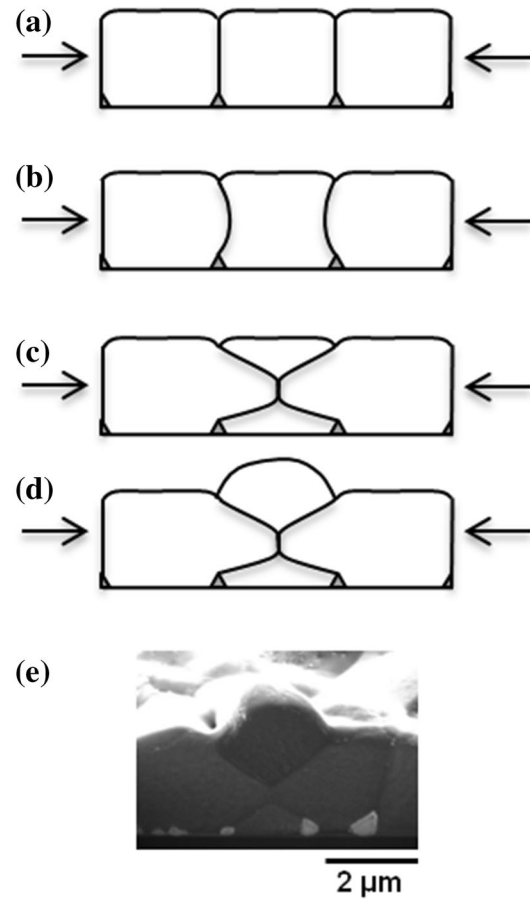

Fig. 4. (a–d) Schematic of proposed whisker nucleation mechanism described in text. (e) Cross-section of nucleus showing microstructure. The figure is adapted with permission from Ref. 17.

top and bottom surface (by the surface roughness and IMC formation, respectively), then the grain boundaries will bow inward as shown in Fig. 4b. Eventually, the boundaries will meet and form a new segment of vertical grain boundary, as well as segments of oblique boundaries with a horizontal component. This results in the creation of a surface grain without needing to nucleate a new grain (Fig. 4c) so that the orientation of the surface grain is the same as the original columnar grain. This site can then grow outward in the form of a whisker or hillock (Fig. 4d). The morphology predicted by this model is consistent with the cross-section of a hillock formed by thermally induced stress shown in Fig. 4e. It is also similar to the morphology beneath whiskers found in IMC studies.[11]

The stress dependence of the nucleation barrier from this mechanism can be calculated from the balance between the strain energy reduced by the grain growth and the increase in the area of the grain boundaries[17] (details of this model can be found in Ref. 37). The resulting barrier to nucleation depends inversely on the stress to the fourth power:

$$\Delta G^*/kT \propto (\sigma_{\text{char}}/\sigma)^4 \qquad (3)$$

A least-squares fit to the behavior in Eq. 3 is shown as the dashed lines in Fig. 3a. The good agreement supports the predicted dependence on σ^{-4}. However, the value of σ_{char} obtained from the fitting does not agree well with the value calculated from reasonable values of the physical constants. This needs to be studied further.

Stress and Temperature Dependence of Whisker Growth Rate

Measurements of Whisker/Hillock Volume Evolution

In addition to the real-time measurements, SEM was used to quantify the size and shape of individual features on the surface after multiple intervals of heating.[35] Figure 5 shows the evolution of the stress and temperature (Fig. 5a) and the feature morphology for several such heating intervals at 45°C (Fig. 5b). The samples were heated at the same rate (2°C/min) as for the uninterrupted measurements. The stress evolution is not significantly changed by the interrupts (i.e., it is similar to the stress evolution during the heating shown in Fig. 2). Multiple surface features (between 14 and 25 for

each temperature) were followed for the different periods of annealing so that the average volume could be determined. Similar measurements were carried out at temperatures of 55°C and 65°C. The growth rate at 75°C was too fast to be able to measure the incremental volume change during heating intervals.

The evolution of the average volume computed from these measurements is shown in Fig. 6a as a function of the heating time. The volume was estimated by assuming that the features had roughly cylindrical geometry and corrected for the angle of the feature relative to the electron beam. The growth rate is clearly not constant and the rate of growth decreases with time. The growth rate at higher temperatures was faster so that shorter heating intervals were used to capture the growth kinetics.

Model for Whisker Growth Rate

The measurements described above allow us to quantify how the stress and the average volume ($\langle V \rangle$) of individual whiskers/hillocks evolve with time. Several important features can be observed from these data. The first is that the growth rate changes with time in a way that is similar way to the average stress in the layer. Furthermore, as the stress approaches a value of approximately -15 MPa, the stress stops relaxing and the whisker stops growing. The growth rate also depends on temperature so that whiskers grow faster at higher temperature for the same stress.

The data suggest the following phenomenological model for the average rate of growth:

$$\mathrm{d}\langle V \rangle / \mathrm{d}t = D(T)\Delta\sigma \qquad (4)$$

where $D(T)$ is a temperature-dependent factor and $\Delta\sigma$ is the average stress above a critical value ($\Delta\sigma = \sigma - \sigma_{\mathrm{cr}}$). A model proposed by Sarobol et al.[27] also has a critical stress and a temperature-dependent growth rate.

We compare this model with the data by plotting the average volume relative to the quantity $\langle \Delta\sigma \rangle \, \Delta t$, where the brackets indicate the measured stress value is averaged over the heating time interval. The results are shown in Fig. 6b. The evolution of the average volume is linear when represented this way, indicating that the model is consistent with the measurements.

The temperature dependence of the growth rate from the parameter $D(T)$ is shown on an Arrhenius plot in Fig. 6c. The linearity suggests that $D(T)$ describes a thermally activated process. The activation energy from the slope is 0.37 eV, similar to the activation energy for grain boundary diffusion
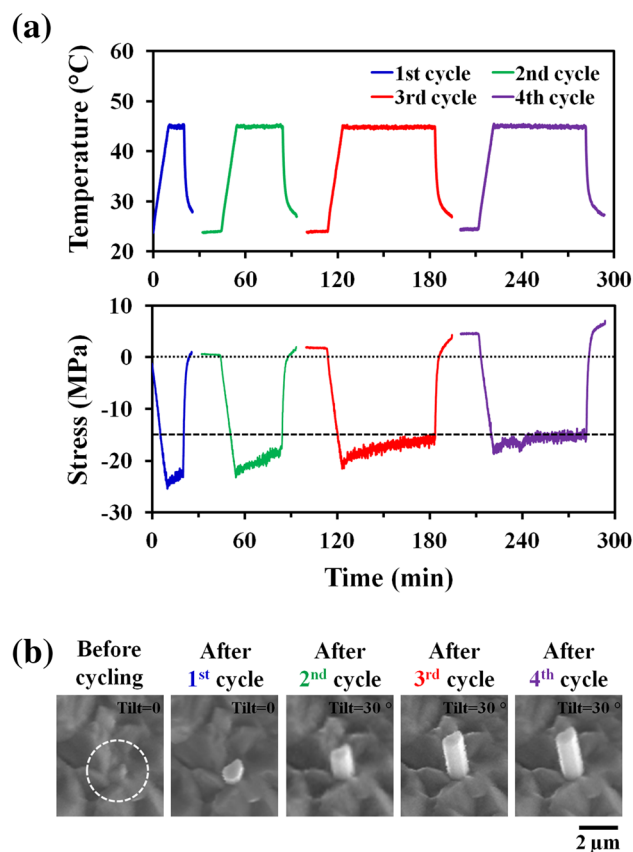

Fig. 5. (a) Temperature and stress evolution during intervals of heating to 45°C. (b) Evolution of typical whisker feature measured via SEM after each heating cycle (Color figure online).
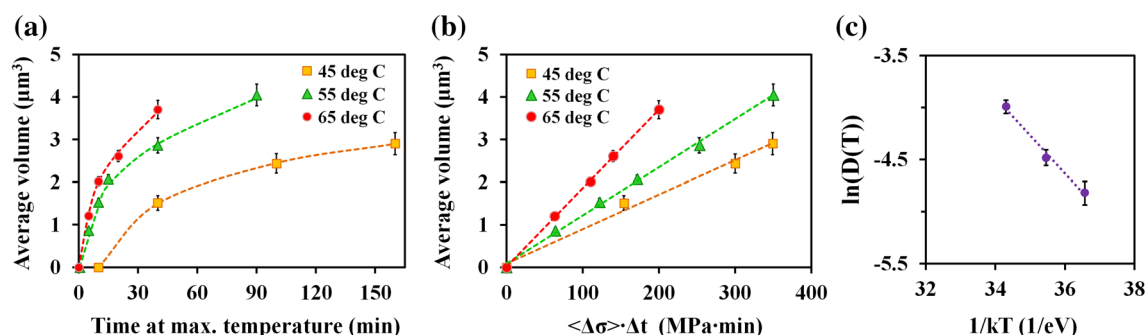

Fig. 6. (a) Average volume of whiskers/hillocks after different time intervals at temperatures indicated in figure. (b) Average volume of whiskers versus the time-averaged stress ($\langle \Delta\sigma \rangle \cdot \Delta t$). (c) Temperature dependence of $D(T)$ on an Arrhenius plot.
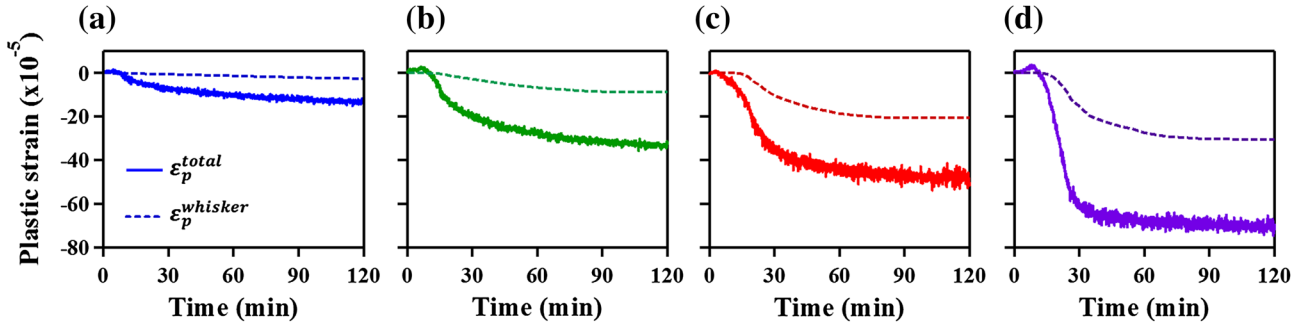
Fig. 7. Measurements of the total plastic strain (solid line) and the estimated plastic strain due to whisker formation (dashed line) for heating to (a) 45°C, (b) 55°C, (c) 65°C, and (d) 75°C.

in Sn.[38,39] This is not surprising because it is known that Sn diffuses over a long range to feed whisker/hillock growth.

We want to emphasize that the analysis above is based only on the average stress and temperature. In other words, we have neglected any long-range spatial variation in the stress across the layer. The good agreement between the model and the data suggests that we can focus on the average stress when considering the driving force for whisker formation, and that the local microstructure does not play the primary role in determining the growth rate (once the feature has nucleated). To investigate this assumption further, we have also performed preliminary finite-element analysis (FEA) calculations of the whisker growth rate[40] that include mechanisms of power–law strain relaxation as well as whisker formation, based on previous work of Buchovecky.[41] These results also show that the whisker growth rate is proportional to the average stress.

Relation Between Whisker Volume and Plastic Strain

The total strain ($\varepsilon_{\text{total}}$) in a thin film is composed of an elastic component (ε_e) and a plastic component (ε_p):

$$\varepsilon_{\text{total}} = \varepsilon_e + \varepsilon_p \quad (5)$$

In the experiments, the total strain is due to the heating and is proportional to the change in temperature (ΔT) and the difference in the CTEs ($\Delta \alpha$). The elastic strain is proportional to the stress (measured by the wafer curvature system) divided by the biaxial modulus of the film (M). Therefore, the plastic strain can be calculated from the measured stress and temperature:[16]

$$\varepsilon_p = \Delta \alpha \Delta T - \frac{\sigma}{M} \quad (6)$$

The evolution of the plastic strain calculated from the measurements for each temperature is shown in Fig. 7. It has a negative value because it corresponds to a compressive stress. Note that it follows similar kinetics to the number of whiskers. It is zero initially (in the elastic regime) and then increases in magnitude when the whiskers start to appear. At a longer time, it saturates at a value that shows more plastic strain for higher temperature.

Plastic strain may arise from multiple processes, so we separate it into a part due to whisker formation ($\varepsilon_p^{\text{whisker}}$) and a part due to other processes (ε_p^o) (e.g., creep and dislocation motion). The change in plastic strain due to whisker formation ($\Delta \varepsilon_p^{\text{whisker}}$) is related to the removal of volume from the layer in the form of the whiskers so that

$$\Delta \varepsilon_p^{\text{whisker}} = \frac{N}{3 V_o} \Delta \langle V \rangle \quad (7)$$

where $\Delta \langle V \rangle$ is the change in the average whisker volume. N and V_o are the number of whiskers and film volume per unit area, respectively. The factor of 3 comes in because the resulting volumetric strain is isotropic.

With Eq. 7, we can estimate how much of the plastic strain is caused by whiskering. We use the measured nucleation density to get N and the growth model to estimate the average whisker/hillock volume. The calculated amount of plastic strain from whisker/hillocks is shown as the dotted line in Fig. 7. At low temperatures, we find that the plastic strain due to whiskers is less than 20% of the total strain, indicating that other relaxation mechanisms are active. At higher temperatures, a larger fraction of the plastic strain can be attributed to whisker formation (approximately 43%), but it is still not the dominant relaxation mechanism. Note that this is similar to the case where the stress is generated by IMC formation. In those studies also,[1] the primary stress relaxation mechanism is not whisker/hillock formation and other mechanisms (dislocation motion and creep) are believed to play the primary role.

We also note that the relative rates of strain relaxation depend on the strain rate. At higher strain rates (not shown), whiskers play a larger role in the strain relaxation. Conversely, for lower strain rates, other relaxation mechanisms besides whiskering are more active.[16]

CONCLUSION

The experiments described above show how thermally induced strain can be used to quantitatively determine the relationship between stress, whisker density, and whisker growth rate. These results suggest that we can understand whisker/hillock formation within the context of a nucleation and growth process where stress is the driving force. To analyze these results, we have made some simplifying assumptions (such as ignoring spatial variations in the stress). In addition, because of the difficulty of measuring the whisker volume and density, there may be errors in the absolute values of the measured volumes used to calculate the whisker-induced strain. However, despite these considerations, we think that these studies reveal much about how the fundamental processes controlling whisker formation operate.

Several useful conclusions can be drawn from this work. The measurements of whisker density highlight the importance of the nucleation process in creating preferred sites where whiskers can start to form. Suppressing the nucleation step can therefore be an important factor in preventing whiskering that we do not feel has received enough attention. However, the suppression of nucleation may also promote the growth of very long whiskers compared to when there are many nucleation sites, so care must be taken. The nucleation rate is seen to depend strongly on the applied stress as well as the temperature. By using classic nucleation theory, we have been able to derive the dependence of the nucleation barrier on stress. We have also proposed a nucleation mechanism based on strain-assisted grain boundary migration that is consistent with the microstructure that we observe at the base of whiskers/hillocks.

The measurements of the growth kinetics enable us to relate the rate of whisker/hillock growth to the average stress in the film. Importantly, we find that the stress must be above a critical value for the feature to grow. This suggests that whiskering can be prevented if the stress can be kept below this value (which depends on the layer microstructure). The temperature dependence of the growth rate is consistent with long-range diffusion along the grain boundaries. Preliminary FEA calculations support the assumption that the growth rate is proportional to the average stress in the layer.

A comparison of the stress evolution with the applied thermal strain enables us to measure the amount of plastic strain relaxation in the film. The combination of the density and volume measurements further allows us to estimate how much of the plastic strain is due to whisker formation. Our results indicate that whiskers are not the primary strain relaxation mechanism in the film, but they become more significant at higher temperatures.

These results provide a framework for understanding how the nucleation rate and growth rate of individual features depends on the stress and temperature. Although further work is still needed, this is a step forward in the eventual development of a comprehensive model for whisker growth.

REFERENCES

1. E. Chason, N. Jadhav, F. Pei, E. Buchovecky, and A.F. Bower, *Prog. Surf. Sci.* 88, 103 (2013).
2. NASA, Tin Whisker (and Other Metal Whisker) Homepage, http://nepp.nasa.gov/whisker/.
3. NASA Engineering and Safety Center, *Technical Assessment Report, National Highway Traffic Safety Administration, Toyota Unintended Acceleration Investigation* (Washington, DC: NASA Engineering and Safety Center, 2011).
4. B. Sood, M. Osterman, and M. Pecht, *Circuit World* 37, 4 (2011).
5. S.M. Arnold, *Paper Presented at the Proceedings of IEEE Electronic Components Technology Conference* (1959), pp. 75–82.
6. R.M. Fisher, L.S. Darken, and K.G. Carroll, *Acta Metall.* 2, 368 (1954).
7. B.Z. Lee and D.N. Lee, *Acta Mater.* 46, 3701 (1998).
8. K.N. Tu, *Phys. Rev. B* 49, 2030 (1994).
9. W.J. Boettinger, C.E. Johnson, L.A. Bendersky, K.W. Moon, M.E. Williams, and G.R. Stafford, *Acta Mater.* 53, 5033 (2005).
10. E. Chason, N. Jadhav, W.L. Chan, L. Reinbold, and K.S. Kumar, *Appl. Phys. Lett.* 92, 171901 (2008).
11. J. Smetana, *IEEE Trans. Electron. Packag. Manuf.* 30, 11 (2007).
12. X. Chen, Z. Yun, C. Fan, and J.A. Abys, *IEEE Trans. Electron. Packag. Manuf.* 28, 31 (2005).
13. C.H. Pitt and R.G. Henning, *J. Appl. Phys.* 35, 459 (1964).
14. K.N. Tu, *Acta Metall.* 21, 347 (1973).
15. Z. Wan, A. Egli, F. Schwager, and N. Brown, *IEEE Trans. Electron. Packag. Manuf.* 28, 85 (2005).
16. F. Pei and E. Chason, *J. Electron. Mater.* 43, 80 (2014).
17. E. Chason, F. Pei, C.L. Briant, H. Kesari, and A.F. Bower, *J. Electron. Mater.* 43, 4435 (2014).
18. F. Pei, C.L. Briant, H. Kesari, A.F. Bower, and E. Chason, *Scripta Mater.* 93, 16 (2014).
19. H.P. Howard, J. Cheng, P.T. Vianco, and J.C.M. Li, *Acta Mater.* 59, 1957–1963 (2011).
20. Y. Mizuguchi, Y. Murakami, S. Tomiya, T. Asai, T. Kiga, and K. Suganuma, *J. Electron. Mater.* 41, 1859 (2012).
21. P. Sarobol, A.E. Pedigo, P. Su, J.E. Blendell, and C.A. Handwerker, *IEEE Trans. Electron. Packag. Manuf.* 33, 159 (2010).
22. N. Jadhav, E. Buchovecky, E. Chason, and A.F. Bower, *JOM* 62, 30 (2010).
23. P. Snugovsky, S. Meschter, Z. Bagheri, E. Kosiba, M. Romansky, and J. Kennedy, *J. Electron. Mater.* 41, 204 (2012).
24. C.-H. Su, H. Chen, H.-Y. Lee, and A.T. Wu, *Appl. Phys. Lett.* 99, 131906 (2011).
25. F. Pei, N. Jadhav, and E. Chason, *JOM* 64, 1176 (2012).
26. M. Sobiech, M. Wohlschlögel, U. Welzel, E.J. Mittemeijer, W. Hügel, A. Seekamp, W. Liu, and G.E. Ice, *Appl. Phys. Lett.* 94, 3 (2009).
27. P. Sarobol, J.E. Blendell, and C.A. Handwerker, *Acta Mater.* 61, 1991 (2013).
28. N. Jadhav, M. Williams, F. Pei, G. Stafford, and E. Chason, *J. Electron. Mater.* 42, 312 (2013).
29. P.T. Vianco and J.A. Rejent, *J. Electron. Mater.* 38, 1815 (2009).
30. P.T. Vianco and J.A. Rejent, *J. Electron. Mater.* 38, 1826 (2009).
31. P. Sarobol, J.P. Koppes, W.H. Chen, P. Su, J.E. Blendell, and C.A. Handwerker, *Mater. Lett.* 99, 76 (2013).

32. F. Pei, N. Jadhav, and E. Chason, *Appl. Phys. Lett.* 100, 221902 (2012).
33. E. Chason, *Thin Solid Films* 526, 1 (2012).
34. L.B. Freund and S. Suresh, *Thin Film Materials: Stress, Defect Formation and Surface Evolution*, 1st ed. (Cambridge: Cambridge University Press, 2009), pp. 86–93.
35. F. Pei, A.F. Bower, and E. Chason, *J. Electron. Mater.* submitted for publication (2015).
36. J.W. Christian, *The Theory of Transformations in Metals and Alloys* (Oxford: Pergamon Press, 1965), pp. 422–479.
37. F.J. Humphreys and M. Hatherly, *Recrystallization and Related Annealing Phenomena* (Oxford: Pergamon, 1995), pp. 207–209.
38. W. Lange and D. Bergner, *Phys. Status Solidi (b)* 2, 1410 (1962).
39. P. Singh and M. Ohring, *J. Appl. Phys.* 56, 899 (1984).
40. F. Pei, E. Buchovecky, A.F. Bower, and E. Chason, Brown University, unpublished research (2015).
41. E. Buchovecky (Ph.D. thesis, School of Engineering, Brown University, 2010).